

Hybrid electrochemical sensor platform for capsaicin determination using coarsely stepped cyclic squarewave voltammetry

Søpstad, S., Imenes, K. & Johannessen, E. A.

Department of Microsystems, Faculty of Technology, Maritime and Natural Sciences,
University of South-Eastern Norway, Borre, Norway

Biosensors & bioelectronics, 130, 374-381.

doi: <http://dx.doi.org/10.1016/j.bios.2018.09.036>

This article has been accepted for publication and undergone full peer review but has not been through the copyediting, typesetting, pagination and proofreading process, which may lead to differences between this version and the Version of Record. This article is protected by copyright. All rights reserved.

1 **Hybrid electrochemical sensor platform for capsaicin determination using coarsely stepped**
2 **cyclic squarewave voltammetry**

3 Sindre Sjøpstad*, Kristin Imenes, Erik A. Johannessen

4 Department of Microsystems, Faculty of Technology, Maritime and Natural Sciences, University
5 of Southeast Norway, Borre, Norway

6 *Corresponding author:

7 E-mail: sso@usn.no, Tel: (0)-(47)-452-77-888

8 **ABSTRACT**

9 A small, standalone electrochemical hybrid sensor platform, combining flexible electronics and
10 screen-printed electrodes, is demonstrated in the determination of capsaicin through adsorptive
11 stripping voltammetry. The sensing scheme was simplified to be compatible with a low-cost
12 device. The simplification involved eliminating the need for additional modification of the
13 electrode and employing a coarsely stepped squarewave voltammetry, a technique which is
14 applicable with less sophisticated instrumentation. This architecture was found to be suitable for
15 concentrations up to at least 5000 μM with a detection limit of 1.98 μM . The screen-printed carbon
16 graphite electrodes were made reusable through an ethanol rinsing protocol. The effect of
17 ethanol/buffer volumetric ratio in the test sample greatly influenced the analytical data, and a fixed
18 10% (v/v) was chosen as a compromise between signal-to-noise ratio and not exceeding the
19 solubility limit of the desired upper range.

20
21 **KEYWORDS:** Capsaicin, electrochemical biosensors, hybrid electronics, chili hotness, screen-
22 printed electrodes

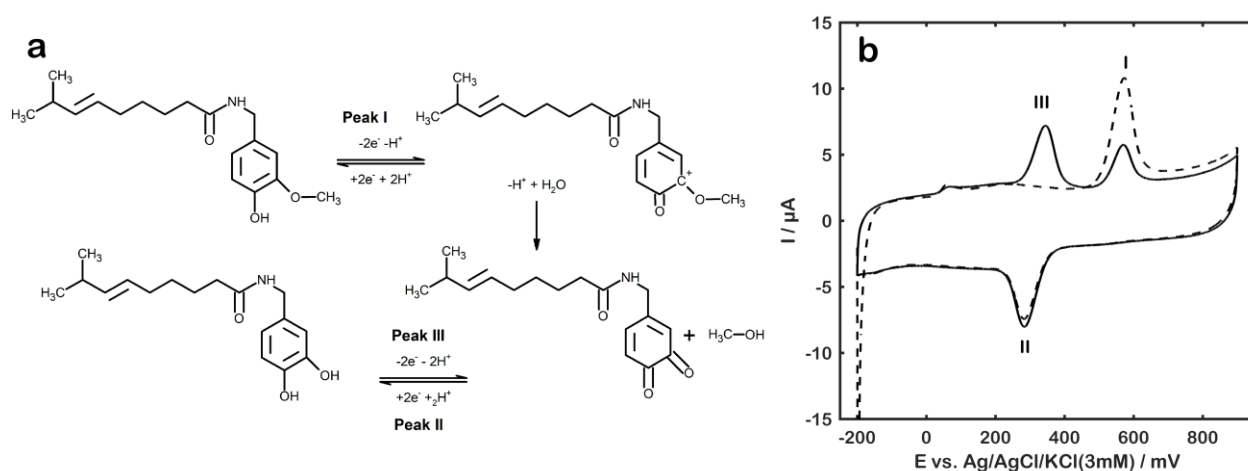
23 **1. Introduction**

1 Capsaicinoids are the chemical compounds responsible for most of the pungency or “hotness”
2 associated with the Capsicum family of plants. The more potent species such as chilies are one of
3 the most popular food additives (Barbero et al., 2008). Capsaicin, the most abundant capsaicinoid,
4 is known for the many positive effects it has on the human health, such as antimutagenic,
5 anticarcinogenic, anti-inflammatory and antitumoral properties (Fattori et al., 2016), It has also
6 been shown to have combative effects on back pains, cholesterol, obesity and gastric
7 (Satyanarayana, 2006). Additionally, it is found in pharmaceutical products such as pain relief
8 dermal patches, ointments and creams. Capsaicin is the active ingredient in weapons used for riot
9 control and pepper spray used for self-defense (Yard and Zühre, 2013). Hence, its use would
10 benefit from an accurate and cheap method for quantifying its content.

11 The hotness of the plant is traditionally measured organoleptically in units of Scoville Heat Units
12 (SHU), and stems from the process of a panel of humans tasting samples at different levels of
13 dilution until the hotness could no longer be tasted (Scoville, 1912). This process is undoubtedly
14 labor intensive and prone to subjective interpretation. In molar quantities the capsaicin may range
15 from sub-nM to, in extreme cases, several hundred mM. The dynamic range is therefore an
16 important performance parameter for an analytical assay in order to limit extensive dilution
17 processes (Edward P Randviir et al., 2013).

18 Electrochemical detection of capsaicin content has therefore been investigated as a cost-effective
19 and simple alternative to more complex techniques, such as high-performance liquid
20 chromatography (HPLC). The sensing scheme for the label-free electrochemical detection of
21 capsaicin was initially proposed by the Compton group (Kachoosangi et al., 2008). They utilized
22 that capsaicin adsorbs to carbon surfaces. By stimulating the adsorbed capsaicin through cyclic
23 voltammetry (CV), also known as adsorptive stripping voltammetry (AdSV), they put it through

1 an EC_{irr}EE reaction scheme. The resulting voltammogram fingerprints the molecule, and the peak
 2 currents (or charge) may be used for quantitative analysis. The process is outlined in Scheme I.
 3 Two cycles are needed, where upon the first ramp, electrooxidation (E) of capsaicin takes place
 4 (peak I). This is immediately followed by an irreversible hydrolysis step (C_{irr}) which transforms
 5 the phenolic group in the structure of capsaicin into a σ -benzenoquinone, and thusly makes up the
 6 oxidized form of the well-known catechol redox couple (Manaia et al., 2012). This redox cycle
 7 (EE) takes place at peaks II and III. Using a screen-printed carbon electrode modified with
 8 multiwalled carbon nanotubes, or MWCNT-SPE, capsaicin could be determined up to at least
 9 35 μ M with a lower limit of detection (LOD) of 0.45 μ M (Kachoosangi et al., 2008).



10
 11 Scheme I. Adsorptive stripping voltammetry (a) reaction pathway, and (b) voltammograms for the first (--) and second
 12 (-) scan.

13 Since this discovery, succeeding literature has focused on expanding the measurable range, with
 14 emphasis on lowering the LOD. In general, this has been achieved through a more complex
 15 modification of the electrode. One exception to this is Ruas de Souza et al., who achieved a $\sim 2x$
 16 sensitivity gain simply by mirroring a screen-printed electrode (SPE) onto the “dead-space” on its
 17 backside, essentially having two sensors on the same footprint (Ruas de Souza et al., 2015),
 18 resulting in LOD of 0.18 μ M. The limitation of this architecture is that the whole sensor has to be
 19 submerged into the test solution (as opposed to dropping small sample volume onto a horizontally

1 oriented, single-sided sensor), requiring higher sample volume, or added liquid handling. Baytak
2 & Aslanoglu developed a sensor to specifically target lower concentrations (0.01 – 0.41 μM) by
3 modifying carbon nanotubes with Ru nanoparticles and applying them a to glassy carbon electrode
4 (Kutluay and Aslanoglu, 2017). Electrochemical impedance spectroscopy was utilized to measure
5 more concentrated capsaicin (up to 4000 μM) with an LOD of 220 μM on screen-printed carbon
6 electrodes modified with CNTs, avoiding the dilution steps required by the original scheme
7 (Edward P Randviir et al., 2013). This was believed to be impossible with CV due to the oxidation
8 peaks merging and shifting outside the potential window of interest, although CV was still found
9 to be the best technique at lower concentrations. EIS however, requires quite complex
10 instrumentation, involving a precise signal generator, phase analyzer etc., which is harder to
11 implement in a simple, low-cost device.

12 The development of a low cost capsaicin detection system would need to share some common
13 traits with existing electrochemical sensors. Many of these are based on screen-printing, which is
14 a scalable and low cost technique for patterning metals and other materials on almost any surface.
15 Thus far, the greatest success story of screen-printed biosensors is that of glucose test strips for
16 diabetes monitoring (Turner, 2013). Flexible electronics has gained considerable attention in the
17 biosensing field due to its many advantages, while benefiting from the scalability, complexity and
18 low cost of the mature rigid printed circuit boards (PCBs). Among its advantages are conformity
19 and light weight. Combining screen-printing with flexible electronics (hybrid technology) may
20 prove a powerful tool in providing conformable, light-weight, and low-cost sensing platforms. The
21 applications range from food safety (both in manufacturing and during storage) and health
22 tracking, to pharmaceuticals manufacturing and environmental monitoring in inaccessible

1 locations such as corrosion monitoring in concrete structures (Abbas et al., 2013; Duffó et al.,
2 2010; Jin et al., 2016) , sensors deployed by drones, or pollution monitoring in oceans and lakes.

3 In this work we present a simplified method for capsaicin detection using unmodified SPEs and
4 coarsely stepped cyclic SWV (CCSWV). This simplification in fabrication and measurement
5 technique allows for better suitability in low-cost sensor platforms while still having the greatest
6 reported range of capsaicin detection for a single technique. Furthermore, we demonstrate a
7 standalone electrochemical detection platform capable of performing this task.

8 **2. Experimental Section**

9 **2.1. Reagents and apparatus**

10 Britton-Robinson (BR) buffer pH 2 and capsaicin stock solution, 0.05 M in ethanol, was
11 acquired from Aliksir Ltd. All other chemicals were purchased from Sigma-Aldrich and were of
12 reagent grade purity. Test solutions with certain capsaicin concentrations were prepared freshly
13 each day. Voltammetric measurements were conducted with a potentiostat (Ana Pot) and screen-
14 printed carbon graphite electrodes (SPREs, A-AC-CAC-203-N), both acquired from
15 Zimmer & Peacock AS. In the case of coarsely stepped SWV, no raw data filtering was employed,
16 as the spiky nature of the peaks would be recognized as anomalies and sought corrected. For CV,
17 a Savitzky-Golay spike rejection filtering was implemented to smooth out any anomalous spikes.
18 3 mM KCl was added to the test samples in order to have the screen-printed reference electrodes
19 (Ag/AgCl) to be operating at a known potential (370 mV vs. SHE), while keeping the analytical
20 signal within the potential window of the device.

21 **2.2. Analytical procedures**

22 A 50 μ L aliquot of sample solution containing different concentrations of capsaicin was
23 dispensed onto the electrodes. The effect of accumulation time has been explored previously

1 (Kachoosangi et al., 2008; Edward P. Randviir et al., 2013; Wang et al., 2016; Yard and Zühre,
2 2013). In general, a higher accumulation time will allow more matter to adsorb to the surface,
3 giving a higher analytical signal and possibly a lower detection limit. On the other hand, the surface
4 will reach maximum coverage at a lower concentration, limiting the sensor's upper detection
5 range. An accumulation time of 60 s at open-circuit potential was chosen for our application. This
6 time was chosen as it provides a convenient mid-point between adsorbing enough analyte to allow
7 detection at lower concentrations, while retaining a high upper detection limit by preventing early
8 surface saturation, and at the same time keeping the protocol execution time down. The open
9 circuit-potential was monitored during this step in an effort to gain additional information about
10 the state of the system without perturbing it. Following the accumulation time, the two cycles of
11 CV or CCSWV was performed. For CV the electrodes were scanned between -200 mV and
12 +900 mV vs. Ag/AgCl/KCl(3mM). For CCSWV the electrodes were scanned between -240 mV
13 and +720 mV with a 60 mV step size and 60 mV amplitude at 3 Hz, resulting in an effective scan
14 rate of 240 mV s⁻¹.

15 The effect of pH has also been thoroughly investigated previously (Ang et al., 2017;
16 Kachoosangi et al., 2008; Wang et al., 2016; Ya et al., 2012a; Yardım, 2011). It has been
17 established that the reaction scheme is pH dependent, and that the reaction pathway is the same in
18 the range pH 1-pH 9. The voltammogram maintains its shape in this range but has a nernstian
19 potential shift along the voltage axis, as well as a reduced signal strength, with increasing pH. The
20 importance therefore lies in maintaining the pH constant, i.e. buffering the sample to reduce the
21 variability, and keeping the pH low for enhanced sensitivity. The acquired buffer was therefore
22 used at its intended low and well-buffered pH 2.

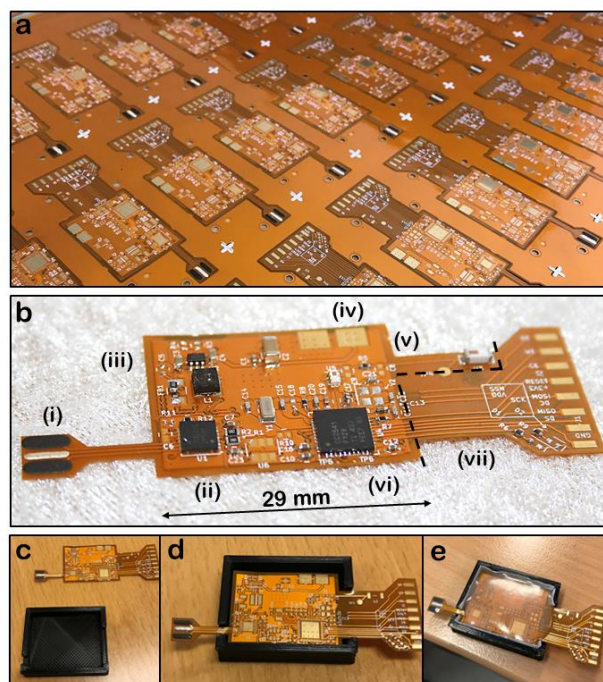
23

2.3. Circuit design

A standalone electrochemical sensor platform with a material cost of about ~25 € was developed in order to realize a low-cost capsaicin-meter (Figure 1). Schematic design and bill of materials can be found in the supplementary material. Although it is being demonstrated for capsaicin detection in this paper, it is intended to be generic platform that permit the use of multiple electrochemical techniques, such as amperometry, coarse voltammetry and open-circuit potentiometry, and can be operated both in continuous and one-shot mode. It is schematically inspired by two application notes from Texas Instruments and Johanson Technology (Johanson Technology, 2012; Singh, 2013), and has been modified into a 4-layer flexible printed circuit board populated with the following main components: A microcontroller (CC2541, Texas Instruments) with built-in Bluetooth low energy (BLE) and analog-to-digital converters was utilized for circuit control, data conversion and wireless data transfer (Figure 1b v-vi). A boost-converter chip (TPS61220, Texas Instruments, Figure 1b iii) was employed to regulate the voltage delivered from the flexible thin-film battery (BV-452229-17ET, Brightvolt LLC). Two analog-front end circuits were used for sensor-readout and conditioning. A chip potentiostat (LMP91000, Texas Instruments, Figure 1b ii) was utilized for voltammetric and amperometric capability, and a unity-gain instrumentation amplifier (MAX4461, Maxim Integrated) for open circuit potentiometric measurements (not used here). Working, reference and counter electrodes were screen-printed directly onto the PCB. The PCB was designed through KiCad EDA (Ver. 2017-07-13, KiCad developers), and manufactured out-of-house (Flexible PCBs, PCBway). The electrodes are placed on their own peninsula (Figure 1b i) to limit splash damage to the electronic components, and to allow free movement of the sensor head, adjusted to conform to the application's requirements. For wearable applications it would be convenient to fold the electrodes such that they are in contact

1 with the skin, while the electronic components are not. For microlitre drop testing the sample
2 would be pipetted directly onto the electrodes. On the opposing side, there is a second peninsula
3 holding pinouts for programming and debugging (Figure 1b vii). Among the debugging
4 functionality is the breakout of the electrodes, so they can be addressed by different
5 instrumentation, effectively bypassing the on-board electronics if required. This is designed such
6 that it can be cut off before deployment to further limit the size of the device. A mold was 3D-
7 printed (Lulzbot TAZ 6, Aleph Products Inc.) to allow encapsulation of the circuit. The mold,
8 depicted in Figure 1c, is a hollow block with openings for both peninsulae (Figure 1d). Conformal
9 silicone coating (3140, Dow Corning Co.) or thermoplastic glue, was poured over the circuit and
10 allowed to cure, forming a water repellant seal around the part of the device holding the electronic
11 components (Figure 1e).

12 In this paper we employed the sensor platform in SWV mode and utilized carbon working and
13 counter electrodes (C2000802P2) and a silver/silver-chloride reference electrode (C2130916D4)
14 from Gwent Electronics Manufacturing Ltd. The electrodes were printed with a semi-automatic
15 screen-printer (DEK 248, ASM Assembly Systems) through steel stencils (SMD Stencils,
16 Pcbway) and cured in a box oven for 30 min. at 60 °C (Figure 1a). The electronic components
17 were manually reflow soldered, after which the circuit was programmed through
18 IAR Embedded Workbench 8051 (IAR Systems). The complete circuit is depicted in Figure 1b.



1
 2 Figure 1. Photograph of electrochemical sensor platform (a) on a 25×25“ panel component assembly and (b) single
 3 sensor platform after assembly. The letters indicate (i) the screen-printed electrodes, (ii) chip potentiostat, (iii) battery
 4 management circuitry, (iv) terminals for flexible battery (dimensions 29×25×0.6 mm) situated on the backside, (v)
 5 antenna circuitry for Bluetooth low energy, (vi) microcontroller with integrated analog-to-digital converter, and (vii)
 6 debug circuitry which can be cut off (--) before deployment. (c-e) Photographs of the encapsulation of the electronics
 7 components in a 3D-printed mold.

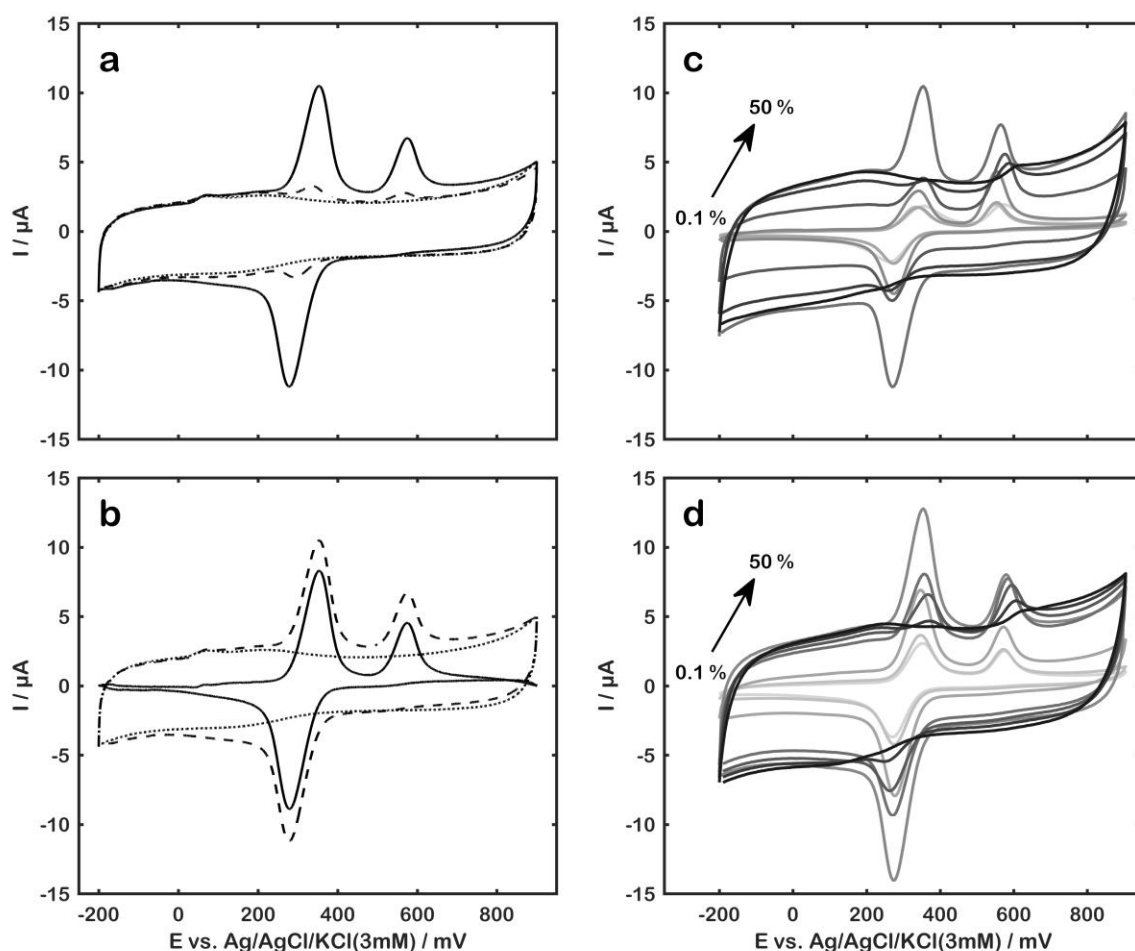
8 3. Results and discussion

9 3.1. Electrode re-usage

10 It is desirable to be able to re-use the electrodes since they constitute a permanent part of the
 11 sensor system that cannot be replaced. Although DI-H₂O previously have been used to rinse the
 12 working electrode between measurements (Kachoosangi et al., 2008; Mpanza et al., 2014), it was
 13 found that this method left residual peaks (Figure 2a), indicating that the substances of the reaction
 14 scheme are still present on the electrode. This would create a falsely high sensitivity if tested under
 15 ascending concentrations of capsaicin and the response would therefore heavily rely on the history
 16 of the electrode, a parameter which would be cumbersome to keep track of in a real application.
 17 Instead, a solution comprising ethanol (>50 % v/v) and buffer was found to effectively remove the
 18 residual peaks, as evidenced by Figure 2a. First, any residual sample was blown off by compressed

1 air. Ethanol-buffer solution was then trickled across the electrodes for around 5 sec, which were
2 held at a ~45 degree angle, using a syringe, followed by evacuating the solution with compressed
3 air. This ritual was repeated a total of three times, consuming about 1 mL of the rinsing solution
4 and 45 seconds of time.

5 A side effect of the ethanol rinse is that the baseline signal (non-peak regions) is magnified. This
6 was remedied by subtracting the baseline signal (no capsaicin) from the signal obtained in the
7 presence of capsaicin, as demonstrated in (Figure 2b). This allowed for easier peak detection,
8 since peaks II and III would originally ride on a shoulder of the blank at lower concentrations.



9
10 Figure 2. (a) Cyclic voltammograms (second scan) in the absence of capsaicin after cleaning by DI-H₂O (--) or
11 ethanol (· ·) following a measurement of 50 μM capsaicin (-). (b) Baseline corrected voltammogram (-) obtained
12 through subtracting the baseline (· ·) from the raw signal (--). (c) The influence of ethanol content (% v/v) at a fixed

1 50 μM capsaicin concentration for fresh and (d) reused electrodes. The ethanol content increases as the shade of the
2 traces darken.

3 **3.2. Ethanol content**

4 Since the capsaicin stock solution had ethanol as the solvent, making up different concentrations
5 in pure buffer solution would consequently change the ethanol content. An investigation was
6 carried out to determine the effect of varying ethanol content. **Figure 2** (c and d) shows the AdSV
7 (2nd cycle) response of different ethanol content under constant 50 μM capsaicin concentration,
8 for both fresh and re-used electrodes. For both kinds of electrodes, at lower concentrations (0.1-1
9 % v/v), the baseline and analytical signal are low, but the signal to baseline ratio (S/B) is high
10 enough to easily distinguish the analytic peaks from the baseline signal. As the ethanol increases
11 (5-20 %), as does the baseline. The peaks ride on-top of this signal, making them easy to spot,
12 especially through the baseline correction mentioned in 3.1. At higher concentrations, the peaks
13 start to retract the into baseline and vanish completely at 50 %. Presumably, this is due to capsaicin
14 being hydrophobic, and prefers to adsorb to carbon when the bulk solution contains primarily
15 water. However, when the solution is rich on ethanol, remaining in the bulk provides a lower
16 energy state, and what little capsaicin is adsorbed is masked by the magnified baseline signal that
17 occurs at higher ethanol concentrations. The presumption is backed by that a concentration greater
18 than 50 % was needed in order to remove any residual peaks, as discussed in 3.1. A second
19 explanation could be that the ethanol content changes the electrical double layer characteristics in
20 such a way the system becomes primarily capacitive, thus prohibiting charge transfer. Indeed, the
21 voltammograms increasingly take on the quasirectangular profile associated with capacitive
22 behavior. Note that one of these hypotheses does not preclude the other.

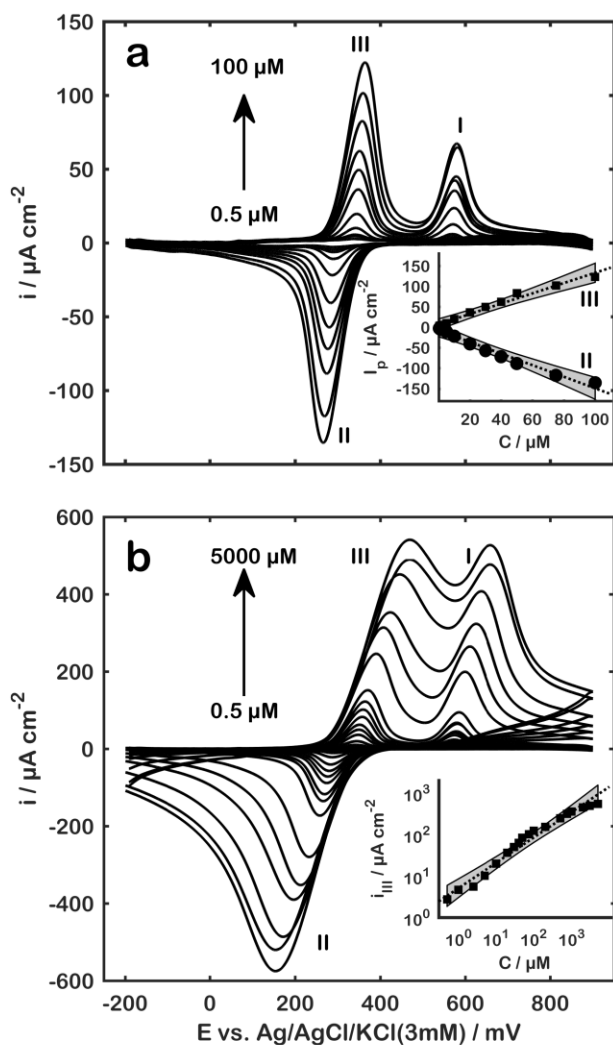
1 In order not to exceed the solubility limit at the highest concentration investigated (5000 μM),
2 and at the same time maintain a high S/B-ratio, a 10 % v/v ethanol was chosen to carry out the
3 quantitative assay.

4 **3.3. Cyclic voltammetry on unmodified carbon electrodes**

5 The voltammogram in **Figure 3** shows the electrochemical response of capsaicin through
6 adsorptive stripping voltammetry for a reused unmodified carbon graphite electrode. A linear
7 region was observed in the range 0.5-100 μM for the second ($I_{II}/\mu\text{A} = -0.0217 \mu\text{A } \mu\text{M}^{-1} - 0.0004$,
8 $N=11$, $R=0.993$) and third peak ($I_{III}/\mu\text{A} = 0.0159 \mu\text{A } \mu\text{M}^{-1} + 0.0650$, $N=24$, $R=0.990$). Their
9 corresponding limits of detection (based on 3σ) were estimated to 0.92 μM and 0.48 μM , and their
10 RSD at a fixed concentration of 10 μM was estimated to 3.7 % and 4.8 % ($N=10$). This
11 performance is in line with that reported for single- and multiwalled CNT modified carbon
12 electrodes (Kachoosangi et al., 2008; Edward P. Randviir et al., 2013). Contrary to these reports,
13 these results suggest that the LOD does not necessarily benefit from employing CNTs, and neither
14 does peak I and III merge when passing the 1000 μM mark, as shown in **Figure 3b**.

15 The data was fitted to linearized forms of nine different adsorption isotherm equations: Linear,
16 Langmuir, Freundlich, Dubinin-Radushkevich (D-R), Temkin, Frumkin, Harkins-Jura, Hasley,
17 Henderson (Başar, 2006). **The linearized adsorption isotherm fits are displayed in the**
18 **supplementary material**. The ones providing the best regression coefficients ($R^2 > 0.9$) were the
19 Langmuir, Freundlich, Hasley, D-R and Henderson. The Freundlich isotherm (log-log plot) was
20 chosen to represent the calibration data as it provides the simplest mathematical treatment (one
21 operation) of the top five fits ($\log I_{III} = -0.032 \times \log[\text{Capsaicin}] - 8.710$, $N=18$, $R^2=0.966$). We
22 attribute the deviation from this model at higher concentrations ($\geq 1000 \mu\text{M}$) to peak I moving
23 outside the potential window and hence not oxidizing all of the adsorbed capsaicin. **However,**

1 through baseline subtraction and an adsorption model, we are able to maintain the LOD while
2 expanding the useable upper range, while eliminating the CTNs from the original ink formulation.

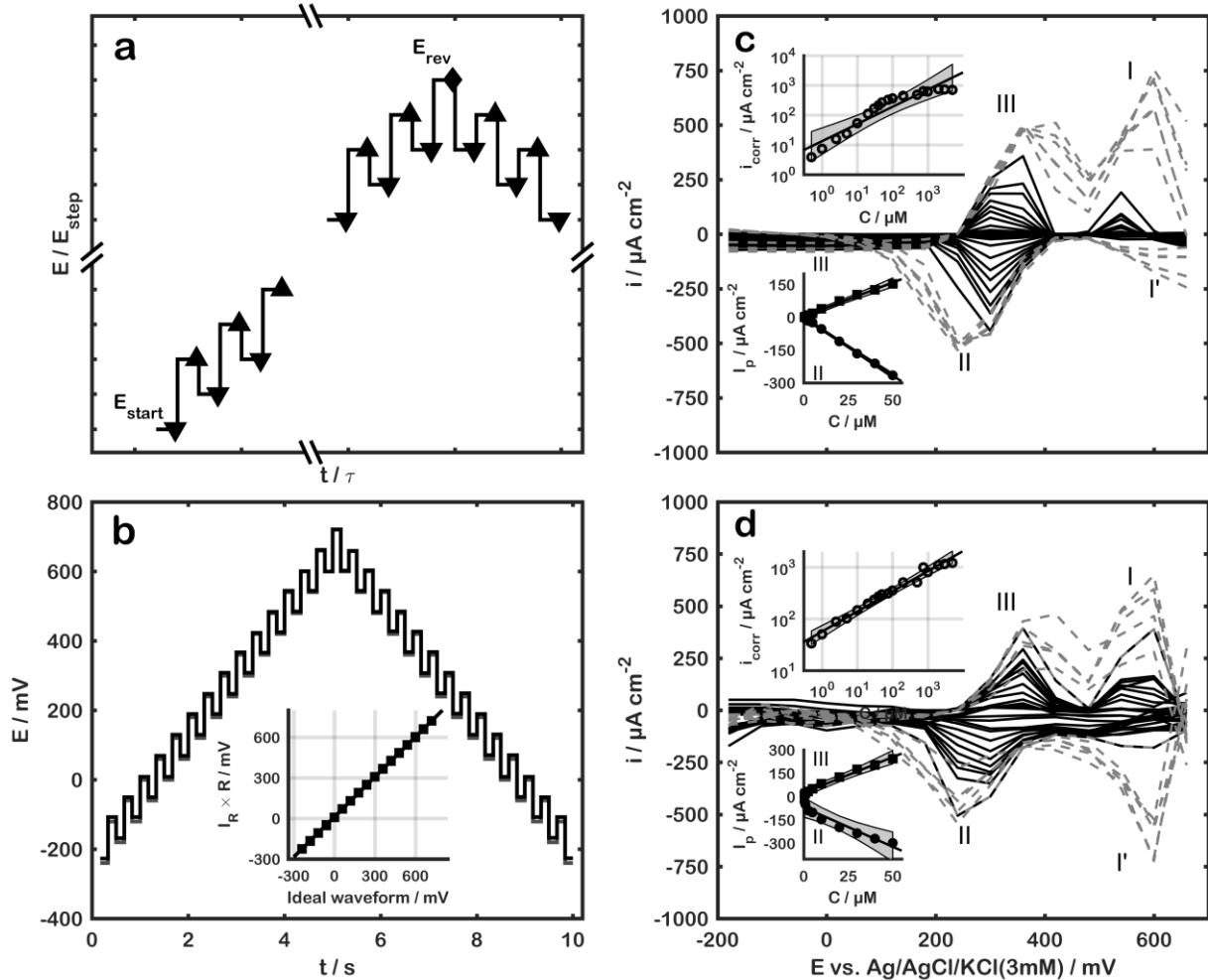


3
4 Figure 3. Baseline subtracted cyclic voltammograms (second scan, 100 mV s^{-1}) for capsaicin concentrations of (a)
5 0.5-100 μM and (b) 0.5-5000 μM on unmodified carbon graphite electrodes. Insets: calibration plots for the peak
6 currents of the second (II) and/or third peaks (III), where the shaded regions represent a confidence interval of 99.9 %.

7 3.4. Coarsely-stepped cyclic squarewave voltammetry

8 SWV was implemented on the sensor platform by cycling through the chip potentiostat's
9 available bias voltage steps, which is programmable from -24 to +24 percent of the supply voltage
10 (3.0 V) in steps of 2 percent, i.e. 60 mV. Therefore, the highest precision waveform that could be
11 generated was a square wave amplitude (E_{amp}) of 60 mV and step height of 60 mV (E_{step}), as

1 depicted in **Figure 4a**. Cruz et al. demonstrated that the LMP91000 could be used for staircase
2 voltammetry (Cruz et al., 2014). This is, to the best of our knowledge, the first time it has been
3 used for SWV, let alone CSWV. The current was sampled immediately before each voltage change
4 step to minimize capacitive contributions, and then transmitted to a smart phone or computer via
5 Bluetooth, allowing for real-time data visualization. To maintain the continuous pulsing, the
6 reversal potential was reused as the first sample on the reverse scan. The waveform was validated
7 by connecting a 4.5 k Ω between the WE and CE/RE terminals, and comparing the current-
8 resistance product with a simulated waveform. Good agreement was found through linear
9 regression ($I_R \times R = 0.978 \text{ E mV} + 10.709 \text{ mV}$, $R^2 = 1.000$, $n = 60$).



1
2 **Figure 4.** Voltage waveform for sensor platform showing (a) where the forward (upward facing triangles), reverse
3 (downward facing triangles), and the shared reverse/forward (diamond) is sampled, and (b) the comparison between
4 a simulated waveform (gray) versus the response of the sensor platform when connected to a 4.5 kΩ resistor (black
5 overlapping the gray). The inset shows the linear regression between the simulated and actual response. (c) **Baseline**
6 **corrected coarse cyclic squarewave voltammograms (second scan) from commercially sourced electrodes and**
7 **potentiostat, and (d) sensor platform with integrated electrodes and electronics. The dotted lines (--) represent the**
8 **signals which satisfies $i_{II} \geq i_{III}$.** The top-left insets in the show the corresponding calibration curves from Eq. (1) and
9 the bottom-left instets displays the sensor's linear ranges. The shaded regions indicate a confidence level of 99.9 %.

10 Capsaicin calibration using CCSWV was carried out with commercially sourced electrodes and
11 potentiostat, and with the developed low-cost sensor platform and integrated electrodes. Their
12 responses are compared in **Figure 4 c and d**. A linear region was identified in the range 0.5-50 μM
13 for the second and third peaks. The LODs for the second peak were estimated to 0.81 μM
14 ($i_{III}/\mu\text{A cm}^{-2} = -5.313 \mu\text{M}^{-1} - 1.204$, N=8, R=0.999) and 1.98 μM
15 ($i_{II}/\mu\text{A cm}^{-2} = -4.963 \mu\text{M}^{-1} - 72.03$, N=8, R=0.931) for commercial electrodes and sensor
16 platform, respectively. The LODs for the third peak were respectively estimated to 2.51 μM

1 ($i_{III}/\mu\text{A cm}^{-2} = 3.109 \mu\text{M}^{-1} + 4.288$, $N=8$, $R=0.992$) and $3.54 \mu\text{M}$
 2 ($i_{III}/\mu\text{A cm}^{-2} = -4.963 \mu\text{A cm}^{-2} \mu\text{M}^{-1} - 72.03$, $N=8$, $R=0.9845$). For the commercial electrodes A
 3 **RSD at a fixed concentration of $10 \mu\text{M}$ was estimated to 4.1 % and 4.7 % ($N=10$) for peaks II and**
 4 **III, while for the sensor platform they were estimated to 9.2 % and 9.9 % ($N=10$).** The slightly
 5 worse performance specs for the LOD for the sensor platform is attributed to the resolution of the
 6 analog-to-digital conversion. At 12-bit resolution and a current range spanning $\pm 214 \mu\text{A}$, the
 7 circuit is only able to discriminate between 104 nA currents at 3.0 V supply voltage. Even so, they
 8 are within one order of magnitude of the original report (Kachoosangi et al., 2008).

9 Due to the limited potential range available with the sensor platform ($\pm 720 \text{ mV}$), the shifting of
 10 the peak potentials with concentration caused the signals to saturate at an earlier time. The
 11 saturation is likely caused by the peak I during the first scan not being able to oxidize all of the
 12 adsorbed capsaicin before the potential is reversed, creating a proportional lowering of peaks II
 13 and III, and hence making them indistinguishable from the lower concentrations. Another
 14 interesting observation is that for these signals, the height of peak I becomes higher than that of
 15 peak III (and II). Furthermore, for these signals, there was an emergence of a peak I', observed
 16 immediately after the potential reversal. All of this combined made possible the criterion for a
 17 correction current, i_{corr} , as described by (1), which enabled the use of the entire range investigated.
 18 The log-log relationship between i_{corr} and capsaicin concentration can be described by
 19 ($\log|i_{corr}/\mu\text{A cm}^{-2}| = 0.578 \log|\mu\text{M}^{-1}| + 1.127$, $N=18$, $R=0.890$) for commercial electrodes and
 20 instrument, and ($\log|i_{corr}/\mu\text{A cm}^{-2}| = 0.390 \log|\mu\text{M}^{-1}| + 1.753$, $N=18$, $R=0.981$) for the sensor
 21 platform. A higher degree of linearity is reached for the sensor platform, meaning that the
 22 corrective current is more effective for this architecture. This is a direct effect of the sensor
 23 platform utilizing continuous pulsing through reusing the current sampled at the reversal potential,
 24 resulting in a greater i' . This is not possible for the commercial potentiostat employed, since CSWV
 25 is not part of its repertoire, and must be implemented by stringing four SWVs. In this case, the
 26 reversal potential is repeated, and the pulsing becomes discontinuous.

$$i_{corr} = \begin{cases} -i_{II} - i_{I'}, & i_I \geq i_{III} \\ -i_{II}, & \text{otherwise} \end{cases} \quad (1)$$

27
 28 **The performance of the sensor platform is compared to other electrode systems in Table I. While**
 29 **it cannot contend with the lower LOD of the more intricate electrode modifications, its dynamic**

- 1 range is superior, and its LOD is in the same order of magnitude as those modified carbon
- 2 nanotubes only.
- 3

Table I. Comparison of the performance of different electrode systems.

Electrode system	Adsorption measurement technique	Utilized range / μM	LOD / μM	Reference
Multiwalled carbon nanotube modified basal plane pyrolytic graphite electrode	Cyclic voltammetry	0.5 – 60	0.31	(Kachoosangi et al., 2008)
Multiwalled carbon nanotube modified basal plane pyrolytic graphite electrode	Cyclic voltammetry	0.5 – 35	0.45	(Kachoosangi et al., 2008)
Boron-doped diamond electrode	Squarewave voltammetry	0.5 – 20	0.034	(Yardim, 2011)
Carbon paste electrode modified with amino-functionalized mesoporous silica	Linear sweep voltammetry	0.04 – 4	0.02	(Ya et al., 2012b)
Singlewalled carbon nanotube paste	Cyclic voltammetry	0 – 34	0.77	(Edward P. Randviir et al., 2013)
Multiwalled carbon nanotube paste	Cyclic voltammetry	0 – 220	1.12	(Edward P. Randviir et al., 2013)
Multiwalled carbon nanotube paste	Electrochemical impedance spectroscopy	0 – 4 000	220	(Edward P. Randviir et al., 2013)
Penil graphite electrode	Squarewave voltammetry	0.016 – 0.32	0.0037	(Yard and Zühre, 2013)
Glassy carbon electrode in ionic liquids	Cyclic voltammetry	0.1 – 10 000	N/A	(Lau et al., 2014)
Glassy carbon electrode modified with gold nanoparticle decorated multiwalled carbon nanotubes	Differential pulse voltammetry	0.15 – 35	0.89	(Mpanza et al., 2014)
Singlewalled carbon nanotube paste in a dual back-to-back electrode configuration	Cyclic voltammetry	5 – 50	0.18	(Ruas de Souza et al., 2015)
Ag/Ag ₂ O nanoparticle/reduced graphene oxide modified electrode	Differential pulse voltammetry	1 – 60	0.40	(Wang et al., 2016)
Ruthenium nanoparticle modified carbon nanotubes on a glassy carbon electrode	Squarewave voltammetry	0.01 – 0.41	0.0025	(Kutluay and Aslanoglu, 2017)
Screen-printed electrode modified with Poly(Na 4-styrenesulfanate) functionalized graphite	Differential pulse voltammetry	0.3 – 70	0.10	(Ang et al., 2017)
Unmodified carbon graphite electrode	Cyclic voltammetry	0.48 – 5000	0.48	This work
Unmodified carbon graphite electrode	Coarse cyclic squarewave voltammetry	0.81– 5000	0.81	This work

Hybrid electrochemical sensor platform with unmodified carbon graphite electrodes

Coarse cyclic squarewave voltammetry

1.98 – 5000

1.98

This work

1

2

3.5. Real samples

The device was tested on chili derived sauces available in Norwegian supermarkets. The sauces were diluted in a 1:2 ratio with ethanol and vortexed for > 1 min to ensure good extraction efficiency, and centrifuged (MiniStar, VWR) at 6000 RPM for 5 min. The supernatant was extracted and mixed with the buffer in a 1:9 ratio, leaving the final solution with a 1:19 ratio between sauce and buffer. All measurements were conducted on the same sensor, employing the rinsing scheme in section 3.1. The following equation was used to convert from concentration to SHU, where c refers to the concentration as calculated from (1) and DF is the ratio of raw sample to total sample volume, which in this case was 20 for all the samples.

$$\text{Scoville heat units} = 15 \frac{\text{SHU}}{\text{ppm}} \times 0.3 \frac{\text{ppm}}{\mu\text{M}} \times c[\mu\text{M}] \times DF^{-1} \quad (2)$$

1 Tabasco Chipotle, Tabasco Pepper and Tabasco Habanero sauces were estimated to have SHU
2 values of 1612, 4044 and 9578 with RSDs 37.5%, 21.9% and 14.1% based on triplicate
3 measurements. The calculated values agree well with the SHU ranges supplied by the
4 manufacturer (McIlhenny Company, n.d.), of 1500-2500, 2500-500 and >7000 for the three
5 respective sauces. In contrast to other reports which uses the standard addition method (spiking
6 the samples with different concentrations of synthetic capsaicin) (Kachosangi et al., 2008;
7 Edward P. Randviir et al., 2013; Wang et al., 2016; Yard and Zühre, 2013; Yardım, 2011), one
8 direct measurement is used here, which greatly simplifies the procedure. The results demonstrated
9 confirms that capsaicin determination can be performed by the proposed low-cost, small, re-usable,
10 hybrid electrochemical sensor platform.

3.6. Additional considerations

One of the clear weaknesses of electrochemical detection is its susceptibility to interference from other electroactive species in the test matrix, which is especially apparent for label-free assays. It is less of an issue in purified foodstuffs like hot sauces, and pharmaceuticals where the capsaicin content is extremely high compared to other interfering species. However, for testing on the actual peppers, the test matrix becomes much more complex due to the plethora of organic compounds present. Two particularly troublesome substances are ascorbic and ferulic acid, since they are oxidizable within the potential window of the AdSV to detect capsaicin, and commonly present in both plants and foodstuffs. Typically, this creates a broadening of the peaks due to redox peak overlap. This has been elegantly solved by way of transfer voltammetry, or medium exchange voltammetry (Yard and Zühre, 2013): In this procedure, the sensor is exposed to the test matrix for a specific time in order to pre-concentrate (accumulate) the capsaicin on the sensor surface. Due to its strong adsorption, the sensor can be removed from the solution and washed with DI-H₂O or buffer solution, removing most of the unwanted electroactive species that do not strongly adsorb while retaining most of the capsaicin. The sensor is then introduced to a pure buffer solution, enabling the stripping voltammetry to be conducted in a more controlled environment, and with many of the potential interference species removed or greatly reduced. This method increases the potential area of applicability for the proposed platform. Chemicals more closely related to capsaicin, e.g. vanillin or other capsaicinoids are more difficult to deal with and their discrimination in adsorptive stripping voltammetry has yet to be solved, as their voltammograms are hard to discriminate from that of capsaicin. The state-of-the art is therefore to report the total capsaicinoid content rather than any quantification of a single capsaicin derivative.

1 Finally, it should be emphasized that this platform is not intended to replace precision laboratory
2 equipment, but rather serve as a bridge for easier deployment of already established and well-
3 known sensor architectures. The fundamental work still needs to be carried out with the best
4 precision available. Only when the sensor has been fully characterized should the decision of being
5 transferred to a low-cost application consisting of a much simpler piece of equipment, like the one
6 presented here, be made.

7 **4. Conclusion**

8 The detection of capsaicin through adsorptive stripping voltammetry on unmodified electrodes
9 was explored for a greater concentration range than previously reported. The lower limit of
10 detection did not suffer significantly from not utilizing carbon nanotubes or other modifying
11 particles in the ink formulation. It was found that deionized water did not completely remove the
12 adsorbed capsaicin derivatives from the electrode surface, and hence, a protocol using ethanol
13 (<50 % v/v) and buffer solution was instigated. The content of ethanol in the sample solution was
14 found to heavily influence both the baseline signal and the height of the analytical peaks, and was
15 therefore fixed to 10 % in order to maximize the detectable range.

16 The detection scheme was successfully applied to a generic sensor platform, built on a
17 25×29 mm flexible, 1.2 g printed circuit board, with integrated battery, potentiostat and Bluetooth
18 low energy communication to a smart phone. The exercise demonstrates that a low-cost, generic
19 electrochemical platform built-from shelf-ware components, is capable of performing the task of
20 more sophisticated laboratory equipment, without much of a loss in performances. Future
21 prospects will seek to utilize the same platform for different analytes and other electrochemical
22 measurement techniques.

23 **Supplementary information**

1 Bill of materials (excel file) and schematic (PDF) for sensor platform. **Figure showing calibration**
2 **data fitted to linearized adsorption isotherms.**

3 4 **Acknowledgements**

5 The authors would like to thank the Norwegian Research Council for funding the work presented
6 in this paper, the Norwegian Nanonetworks Ph.D. network for an external fabrication grant,
7 Zimmer and Peacock AS (ZP) and Aliksir Ltd for providing consumables and access to facilities,
8 Dr. Ahn Tuan Nguyen (USN) for advice in the design of flexible electronics, Dr. Thi Thuy Luu
9 (ZP) and Denis Puskar (ZP) for assistance in designing the 3D-printed mold and a custom 3D-
10 printed edge connector for the sensor platform, **and Prof. Ulrik Hanke (USN) for inspiring a**
11 **mechanistic investigation into the sensor response.**

12 13 **REFERENCES**

- 14 Abbas, Y., Olthuis, W., Van Den Berg, A., 2013. A chronopotentiometric approach for
15 measuring chloride ion concentration. *Sensors Actuators, B Chem.* 188, 433–439.
16 <https://doi.org/10.1016/j.snb.2013.07.046>
- 17 Ang, Y.W., Uang, B.H., Ai, W.D., Bin, X.U., 2017. Sensitive Electrochemical Capsaicin
18 Sensor Based on a Screen Printed Electrode Modified with Poly (sodium 4-
19 styrenesulfonate) Functionalized Graphite 33, 793–799.
- 20 Barbero, G.F., Liazid, A., Palma, M., Barroso, C.G., 2008. Fast determination of
21 capsaicinoids from peppers by high-performance liquid chromatography using a
22 reversed phase monolithic column. *Food Chem.* 107, 1276–1282.
23 <https://doi.org/10.1016/j.foodchem.2007.06.065>
- 24 Başar, C.A., 2006. Applicability of the various adsorption models of three dyes
25 adsorption onto activated carbon prepared waste apricot. *J. Hazard. Mater.* 135,
26 232–241. <https://doi.org/10.1016/j.jhazmat.2005.11.055>
- 27 Cruz, A.F.D., Norena, N., Kaushik, A., Bhansali, S., 2014. A low-cost miniaturized
28 potentiostat for point-of-care diagnosis. *Biosens. Bioelectron.* 62, 249–254.
29 <https://doi.org/10.1016/j.bios.2014.06.053>
- 30 Duffó, G.S., Farina, S.B., Giordano, C.M., 2010. Characterization of solid embeddable
31 reference electrodes for corrosion monitoring in reinforced concrete structures.
32 *Mater. Corros.* 61, 480–489. <https://doi.org/10.1002/maco.200905346>

1 Fattori, V., Hohmann, M., Rossaneis, A., Pinho-Ribeiro, F., Verri, W., 2016. Capsaicin:
2 Current Understanding of Its Mechanisms and Therapy of Pain and Other Pre-
3 Clinical and Clinical Uses. *Molecules* 21, 844.
4 <https://doi.org/10.3390/molecules21070844>

5 Jin, M., Jiang, L., Xu, J., Chu, H., Tao, D., Bai, S., Jia, Y., 2016. Electrochemical
6 Characterization of Solid Ag/AgCl Reference Electrode with Different Electrolytes
7 for Corrosion Monitoring of Steel in Concrete. *Electrochem. Soc. Japan* 2, 383–
8 389. <https://doi.org/http://dx.doi.org/10.5796/electrochemistry.84.383>

9 Johanson Technology, 2012. Johanson Technology, Inc. Highly temperature-stable
10 Impedance Matched RF Front End Differential Balun-Low Pass Filter Integrated
11 Ceramic Component [WWW Document]. URL
12 [https://www.johansontechnology.com/2450bm15a0002-matched-balun-for-t-i-253x-](https://www.johansontechnology.com/2450bm15a0002-matched-balun-for-t-i-253x-family-chipsets)
13 [family-chipsets](https://www.johansontechnology.com/2450bm15a0002-matched-balun-for-t-i-253x-family-chipsets)

14 Kachoosangi, R.T., Wildgoose, G.G., Compton, R.G., 2008. Carbon nanotube-based
15 electrochemical sensors for quantifying the “heat” of chilli peppers: the adsorptive
16 stripping voltammetric determination of capsaicin. *Analyst* 133, 888.
17 <https://doi.org/10.1039/b803588a>

18 Kutluay, A., Aslanoglu, M., 2017. Sensitive determination of capsaicin in pepper
19 samples using a voltammetric platform based on carbon nanotubes and ruthenium
20 nanoparticles. *Food Chem.* 228, 152–157.
21 <https://doi.org/10.1016/j.foodchem.2017.01.161>

22 Lau, B.B.Y., Panchompoo, J., Aldous, L., 2014. Extraction and electrochemical
23 detection of capsaicin and ascorbic acid from fresh chilli using ionic liquids. *New J.*
24 *Chem.* <https://doi.org/10.1039/C4NJ01416B>

25 Manaia, M.A.N., Diculescu, V.C., Gil, E.D.S., Oliveira-Brett, A.M., 2012. Guaicolc
26 spices curcumin and capsaicin electrochemical oxidation behaviour at a glassy
27 carbon electrode. *J. Electroanal. Chem.* 682, 83–89.
28 <https://doi.org/10.1016/j.jelechem.2012.06.023>

29 McIlhenny Company, n.d. Scoville Chart [WWW Document]. URL
30 <https://www.tabasco.com/product/chipotle-sauce/> (accessed 8.8.18).

31 Mpanza, T., Sabela, M.I., Mathenjwa, S.S., Kanchi, S., Bisetty, K., 2014.

1 Electrochemical determination of capsaicin and silymarin using a glassy carbon
2 electrode modified by gold nanoparticle decorated multilayered carbon nanotubes.
3 *Sensors* 2813–2828. <https://doi.org/10.1080/00032719.2014.924010>

4 Randviir, E.P., Metters, J.P., Stainton, J., Banks, C.E., 2013. Electrochemical
5 impedance spectroscopy versus cyclic voltammetry for the electroanalytical
6 sensing of capsaicin utilising screen printed carbon nanotube electrodes †.
7 <https://doi.org/10.1039/c3an00368j>

8 Randviir, E.P., Metters, J.P., Stainton, J., Banks, C.E., 2013. Electrochemical
9 impedance spectroscopy versus cyclic voltammetry for the electroanalytical
10 sensing of capsaicin utilising screen printed carbon nanotube electrodes. *Analyst*
11 138, 2970. <https://doi.org/10.1039/c3an00368j>

12 Ruas de Souza, A.P., Bertotti, M., Foster, C.W., Banks, C.E., 2015. Back-to-Back
13 Screen-Printed Electroanalytical Sensors: Extending the Potential Applications of
14 the Simplistic Design. *Electroanalysis* 27, 2295–2301.
15 <https://doi.org/10.1002/elan.201500155>

16 Satyanarayana, M.N., 2006. Capsaicin and gastric ulcers. *Crit. Rev. Food Sci. Nutr.* 46,
17 275–328. <https://doi.org/10.1080/1040-830491379236>

18 Scoville, W., 1912. Note on capsicum. *Am. Pharm. Assoc.* 1, 453–454.
19 <https://doi.org/DOI:10.1002/jps.3080010520>

20 Singh, A., 2013. Gas Sensor Platform Reference Design.

21 Turner, A.P.F., 2013. Biosensors: sense and sensibility. *Chem. Soc. Rev.* 42, 3184.
22 <https://doi.org/10.1039/c3cs35528d>

23 Wang, Y., Huang, B., Dai, W., Ye, J., Xu, B., 2016. Sensitive determination of capsaicin
24 on Ag/Ag₂O nanoparticles / reduced graphene oxide modified screen-printed
25 electrode. *JEAC* 776, 93–100. <https://doi.org/10.1016/j.jelechem.2016.06.031>

26 Ya, Y., Mo, L., Wang, T., Fan, Y., Liao, J., Chen, Z., Manoj, K.S., Fang, F., Li, C., Liang,
27 J., 2012a. Highly sensitive determination of capsaicin using a carbon paste
28 electrode modified with amino-functionalized mesoporous silica. *Colloids Surfaces*
29 *B Biointerfaces* 95, 90–95. <https://doi.org/10.1016/j.colsurfb.2012.02.025>

30 Ya, Y., Mo, L., Wang, T., Fan, Y., Liao, J., Chen, Z., Srivastava, K., Fang, F., Li, C.,
31 Liang, J., 2012b. Highly sensitive determination of capsaicin using a carbon paste

1 electrode modified with amino-functionalized mesoporous silica. *Colloids Surfaces*
2 *B Biointerfaces* 95, 90–95. <https://doi.org/10.1016/j.colsurfb.2012.02.025>
3 Yard, Y., Zühre, Ş., 2013. Electrochemical evaluation and adsorptive stripping
4 voltammetric determination of capsaicin or dihydrocapsaicin on a disposable pencil
5 graphite electrode. *Talanta* 112, 11–19.
6 <https://doi.org/10.1016/j.talanta.2013.03.047>
7 Yardım, Y., 2011. Sensitive Detection of Capsaicin by Adsorptive Stripping Voltammetry
8 at a Boron-Doped Diamond Electrode in the Presence of Sodium Dodecylsulfate.
9 *Electroanalysis*.
10